Suppression of Harmonics in Microstrip Filters with Stagger Tuning and Voltage Redistributions

Huang, Frederick

DOI:
10.1109/TMTT.2014.2303939

Document Version
Early version, also known as pre-print

Citation for published version (Harvard):
Huang, F 2014, 'Suppression of Harmonics in Microstrip Filters with Stagger Tuning and Voltage Redistributions', *IEEE Transactions on Microwave Theory and Techniques*, vol. 62, no. 3, 10.1109/TMTT.2014.2303939, pp. 464-471. https://doi.org/10.1109/TMTT.2014.2303939

 IEEE Trans. on Microwave Theory and Techniques, vol. 62, no. 3, pp. 464-471, Mar 2014.
DOI 10.1109/TMTT.2014.2303939. Available on IEEE Xplore.

Suppression of Harmonics in Microstrip Filters with Stagger Tuning and Voltage Redistributions

Frederick Huang

***Abstract*— The stop bands of microstrip filters were extended by additional stubs to alter the resonant frequencies of the 2nd and 3rd harmonics, making the resonators stagger tuned. The stubs also change the voltage distributions in the resonators, modifying the coupling coefficients. Equations for estimating the frequency shifts are given, and the operating principle of the voltage redistributions is discussed. Harmonics were suppressed to better than -34 dB in measured filters with 22%, 15%, and 8% bandwidth, with no measurable increase in passband attenuation.**

***Index Terms*—harmonic suppression, microstrip filters, spurious response suppression, stubs.**

I. Introduction

THE UPPER stop band of microstrip filters is often limited by harmonic or other spurious responses. The second harmonic can be suppressed either by introducing Bragg reflections at the second harmonic or equalizing the odd and even modes of the coupled sections, with indentations or variations in width in the microstrip [1]-[5]. Alternatives are additional inductors [6], ground plane apertures [7], [8] or ground plane resonators [9]. The Bragg reflections can also be used for higher order harmonics [5]. Spurious responses can also be shifted to higher frequencies [10], [11] using step-impedance resonators. Resistive attenuation that is significant only in specific resonator modes has also been used [12]-[14]. An alternative is for the resonators to have the same fundamental but differing higher order resonances [15]-[17], or, stagger tuned spurious peaks. Stubs or other resonators can also be added to the main resonators, to shift the frequencies of the spurious responses [18],[19]. The stubs may introduce transmission zeroes that suppress the spurious responses[20],[21], but additional resonances may be introduced and these have to be stagger tuned. Finally, the overlap between resonators can be varied to eliminate coupling at the harmonic frequencies [22]-[24].

In this paper, stubs, approximately quarter wavelength at the third harmonic, are added so that the 2nd and 3rd resonances are different between resonators. An improvement on [18],[19] is that the stubs are specifically designed so that the resonant peaks are well spaced in the stop band, to make full use of the technique. This work differs from [15]-[17] in that the main part of the resonators is not changed compared with the original filter, except for some minor readjustment to maintain the filter characteristics. Thus if the original filter was designed with step impedance resonators for compactness, or with wide tracks for low sensitivity to fabrication over-etch, then at least all the main lines can remain as such. The work extends [18], [19] by shifting both the 2nd and 3rd harmonics using a single asymmetrically placed stub, and investigates the resulting change in coupling coefficient. It draws on [14], but depends on the stagger tuning instead of the resistive load.

The relatively simple structure allows equations to be formulated to design the characteristic impedances and tap positions of the stubs, and these are confirmed by comparisons with simulations. An equation for the change in coupling coefficients caused by the stubs is also provided as they affect the level of the spurious peaks. It is found to be reasonable under idealized conditions. However in the final filters, with spurious responses reduced to the -35 or -40 dB level, the estimate is easily upset by additional long-range coupling and other factors to be discussed, so it is inaccurate. Its use is to illustrate the principle of operation, and possibly to form part of a future, more comprehensive theory. The equations for the change in coupling coefficient are believed to be new and may also be relevant to stubs in dual mode resonators [25] and dual-band filters [26],[27].

One of the harmonic-suppressed filters is shown in fig. 1. Before the addition of the stubs to hairpins B and D, simulations of current densities at the 2nd and 3rd harmonics show large currents only in resonators *B*, *C*, and *D*, while *A* and *E* are damped by the input and output. These responses each show three peaks, which also suggests that only 3 resonators are active. Thus, the resonances of *A* and *E* are very broad and shifting them is useless. Stubs are added only to *B* and *D* to make them differ from *C*. The description also assumes third order harmonic responses, although it can easily be generalized to higher orders.

Hairpin filters with fractional bandwidths of 22%, 15%, and 8% were fabricated to show that a wide range of bandwidths can be accommodated.

Submitted 14 Sep 2013.

F. Huang is with the University of Birmingham, UK, (phone: UK (0)121-4144299; fax: UK (0)121-4144291; e-mail: f.huang@bham.ac.uk).

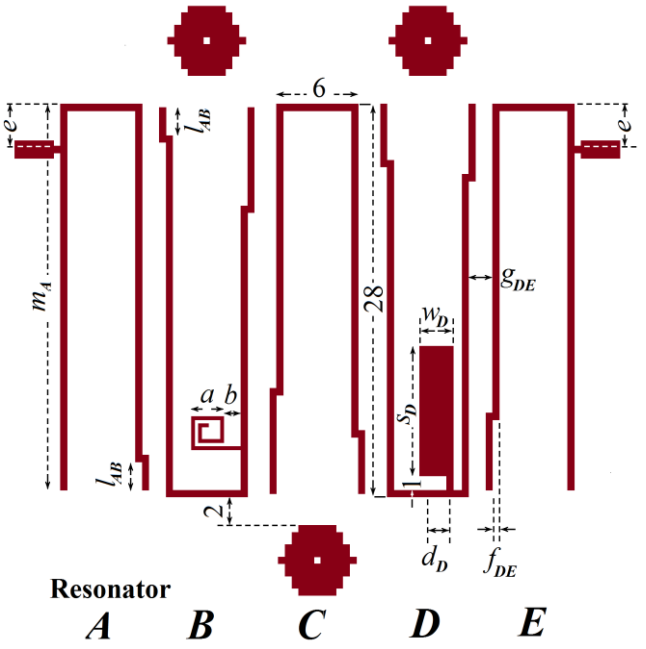

Fig. 1. Example of a 5th order hairpin microstrip filter with stubs attached to resonators *B* and *D*. Dimensions in mm. Drawn to scale for the 8% bandwidth filter to be described.

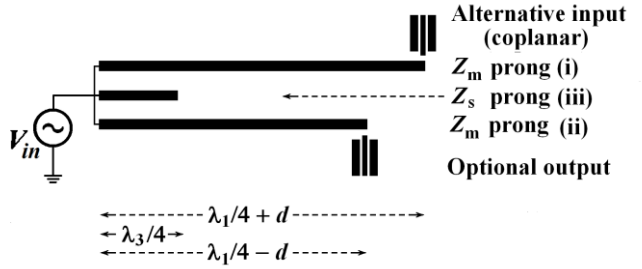

Fig. 2. Transmission line model of a resonator and stub. λ_1 and λ_3 are the wavelengths at the fundamental and the third harmonic.

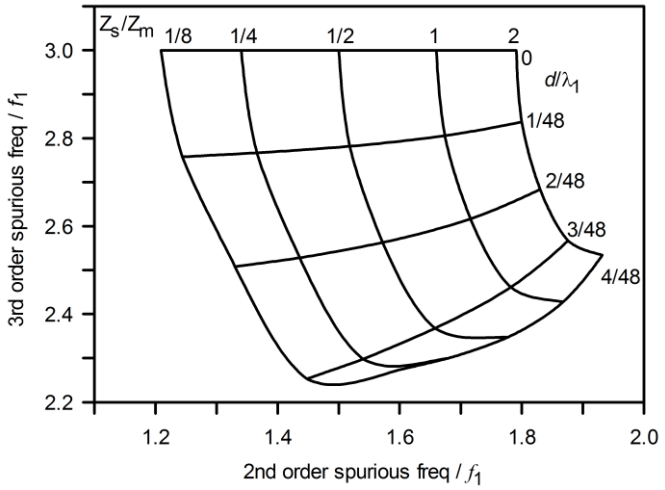

Fig. 3. Estimated frequency shifts of the 2nd and 3rd order spurious frequency due to the stub.

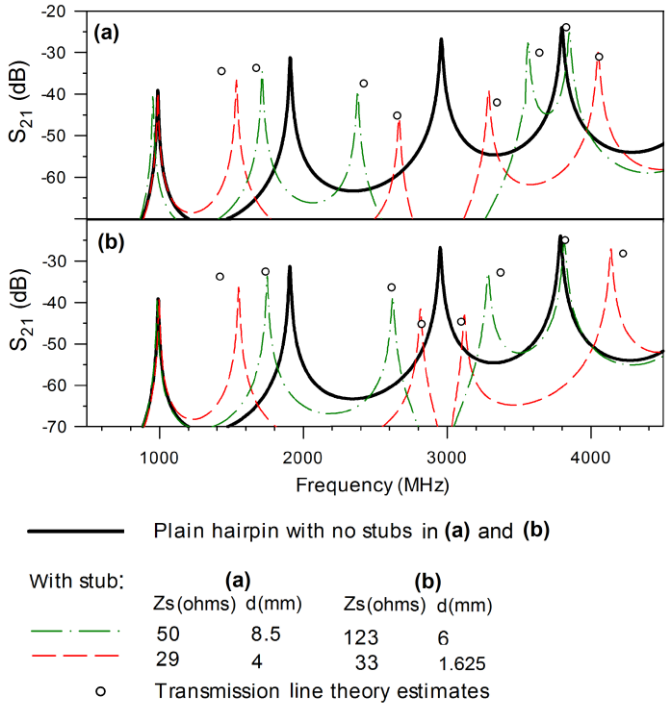

Fig. 4. Simulated S_{21} of single resonators with and without stubs, similar to resonators B, C, or D in fig. 1 Weak external coupling via coplanar lines is provided as in fig. 2. The responses are compared with the transmission line theory estimates of attenuation and resonance frequency. The main line characteristic impedance is Z_m = 72 ohms and $\lambda_1/2$=61mm . See section II for more details.

II. Frequency Shift due to Stubs

The transmission line model of a resonator with a stub is shown in fig. 2. Prongs (*i*) and (*ii*) form the main line, with total length $\lambda_1/2$, that is half a wavelength at the fundamental frequency. Prong (*iii*) is the additional stub with length $\lambda_3/4$ where the third harmonic wavelength is nominally $\lambda_3 = \lambda_1/3$. The tap position is a small distance d from the center of the resonator, the voltage minimum at the fundamental, so the stub has little effect [14]. At the second harmonic, the tap is close to a voltage maximum, so it loads the main resonator, and the resonance shifts from f_2 to f_{21} by an amount Δf_{21}. At the third harmonic f_3, the stub resonates so it has a large effect, splitting f_3 into two peaks f_{31} and f_{32}, shifted by Δf_{31} and Δf_{32} from the original position of f_3.

The principles in the analysis are similar to [27]. The input admittances of the three prongs are

$$Y_i = \frac{j}{Z_m}\tan\left[2\pi\frac{f}{f_1}\left(\frac{1}{4}+\frac{d}{\lambda_1}\right)\right] \quad (1)$$

$$Y_{ii} = \frac{j}{Z_m}\tan\left[2\pi\frac{f}{f_1}\left(\frac{1}{4}-\frac{d}{\lambda_1}\right)\right] \quad (2)$$

$$Y_{iii} = \frac{j}{Z_s}\tan\left[\frac{\pi}{6}\frac{f}{f_1}\right] \quad (3)$$

where f_1, Z_m, and Z_s are the fundamental resonance, the characteristic impedance of the main line, and that of the stub. The resonance condition is

$$Y_i + Y_{ii} + Y_{iii} = 0 \quad (4)$$

The resonances were found numerically, and shown in fig. 3 for variable d and Z_s. $|\Delta f_{31}|$, and $|\Delta f_{32}|$ are not exactly equal, and the vertical axis is based on an average value,

$$f'_{31} = \frac{f_3 - 0.5(|\Delta f_{31}| + |\Delta f_{32}|)}{f_1} \quad (5)$$

This quantity is more useful than f_{31} and f_{32} because $|\Delta f_{31}|$ and $|\Delta f_{32}|$ can be adjusted to be equal by varying the stub length. The graph shows that Δf_{21} and Δf_{31}' can be varied independently by choice of Z_s and d.

The estimated frequency shifts for four specific cases are compared with "SONNET" 0.125 mm cell size, "edge mesh" electromagnetic simulations in fig. 4. These simulations have a 1.27 mm thick substrate with dielectric constant 10.2 and loss tangent 0.0023. The hairpins are 72 ohm lines with a track width of 0.5 mm. They resemble resonator B, C, or D in fig. 1, measuring 6mm x 28 mm with distance f_{DE} = 0. The 29, 33, and 50 ohm stubs have widths 3, 2.5, and 1.25 mm, and lengths 7.125, 7.25, and 7.75 mm respectively. They are somewhat shorter than $\lambda_3/4$ because of the narrow taps similar to resonator D in fig. 1, included to minimize the perturbation of the electromagnetic fields near the main line. The values of Z_m and Z_s were found from SONNET, since the software was already being used, but with "fine mesh" and a cell size of 0.125 mm. Because of the good handling of current crowding at the microstrip edges, the values are only marginally high compared with similar computations using a finer mesh. A square spiral with track width 0.25 mm, side a=2.375 mm, and lead b=1.25 mm (fig. 1) was found from simulations to be equivalent to a 123 ohm straight stub, and used for this stub because the line width is wider and easier to fabricate. In the simulations, input and output are coplanar lines, which can be made narrow (centre line is 0.25 mm wide, and gaps are 0.125 mm), as required in section III.

The transmission line estimates accept the simulated values of f_2, f_3, and f_4, and use the above equations only to find the shifts f_{21}/ f_2 etc. They show quite good agreement except for the left-most peaks. A simulation without the narrow taps was performed to observe any difference caused by the bottleneck. Other simulations with the stub on the outside instead of within the "U" of the hairpin, and at right angles to the main line were also done to observe the effect of reducing the capacitive and inductive coupling between the stub and the main line. The frequency errors of these left-most peaks have a similar magnitude to the shifts caused by the narrow taps and the capacitive and inductive coupling.

III. The Effect of Voltage Redistribution on Coupling Coefficient

The voltage along prong (i) has the form

$$V_i(z) = V_1 \cos\left[2\pi \frac{fz}{v}\right] \quad (6)$$

where position z is measured from the right-hand end and v is the propagation velocity. The exp(jωt) time dependence has been omitted for brevity. V_1 is the potential at the right-hand end. At the left-hand end,

$$V_{in} = V_1 \cos\left[2\pi \frac{f}{f_1}\left(\frac{1}{4} + \frac{d}{\lambda_1}\right)\right] \quad (7)$$

and the energy in the electric field associated with prong (i) is

$$U_i = \frac{V_{in}^2}{2Z_m v} \sec^2\left[2\pi \frac{f}{f_1}\left(\frac{1}{4} + \frac{d}{\lambda_1}\right)\right] \int \cos^2\left[2\pi \frac{fz}{v}\right] dz \quad (8)$$

where the integration should be made over the whole prong. Similar equations can be found for U_{ii} and U_{iii} in the other prongs. The total energy is

$$U = U_i + U_{ii} + U_{iii}\,. \quad (9)$$

From (7) - (9), the quantity $V_1/\sqrt{U}$ can be found, with V_{in} eliminated. The corresponding value $V_0/\sqrt{U_0}$ for a resonator with no stub can be found similarly. The ratio

$$n_i = \frac{V_1/\sqrt{U}}{V_0/\sqrt{U_0}} \quad (10a)$$

gives the change in voltage in prong (i) compared with a resonator with no stub; it affects the coupling coefficient and hence the level of the spurious responses. It is modeled as an ideal transformer with turns ratio 1:n_i, where n_i is not necessarily an integer. Correspondingly for prong (ii),

$$n_{ii} = \frac{V_2/\sqrt{U}}{V_0/\sqrt{U_0}} \quad (10b)$$

The resulting equivalent circuit for resonator B in one of the fifth order filters is shown in fig. 5(a). Normalized values are taken, so that L_B=C_B=1/(1+$\Delta\omega_B$), and $\Delta\omega_B$ is the fractional resonance frequency shift described in the previous section. Since resonator A is inactive at the 2nd and 3rd order spurious peaks, it is regarded as part of the coupling structure to the external circuit. The original external Q factor is Q_e= 1/k_e, and k_e is the "external coupling coefficient". As seen from the LC circuit, the source impedance is 1/(k_e n_{Bi}^2), so the new external coupling coefficient is k_e n_{Bi}^2.

On the right hand side of fig. 5, the second transformer can be combined with the immitance inverter which represents the coupling coefficient k between B and C, and the combined ABCD matrix is

$$\begin{bmatrix} \frac{1}{n_{Bii}} & 0 \\ 0 & n_{Bii} \end{bmatrix} \begin{bmatrix} 0 & \frac{1}{j\omega k} \\ j\omega k & 0 \end{bmatrix} = \begin{bmatrix} 0 & \frac{1}{j\omega k n_{Bii}} \\ j\omega k n_{Bii} & 0 \end{bmatrix} \quad (11)$$

This is an immitance inverter with capacitor value k n_{Bii}. If resonator C (not shown) to the right of the immitance inverter includes an n_{Ci}:1 transformer, this can also combine with the immitance inverter, and the new coupling coefficient between

B and C is $k\, n_{Bii}\, n_{Ci.}$ Combined electric and magnetic coupling is not considered, but an equivalent circuit is suggested in fig. 5(b). The main feature is the differing turns ratios, $1{:}n_{Bii}$ and $n_{Bii}{:}1$. Voltage is stepped up (for $n_{Bii}>1$) by one transformer while current is stepped up by the other.

For a constant total energy U, V_1 can only be increased by a factor of less than approximately $\sqrt{2}$ (for small d), while V_2 is reduced virtually to zero (or vice versa). The overall effect is to decrease coupling coefficients, and hence the spurious responses.

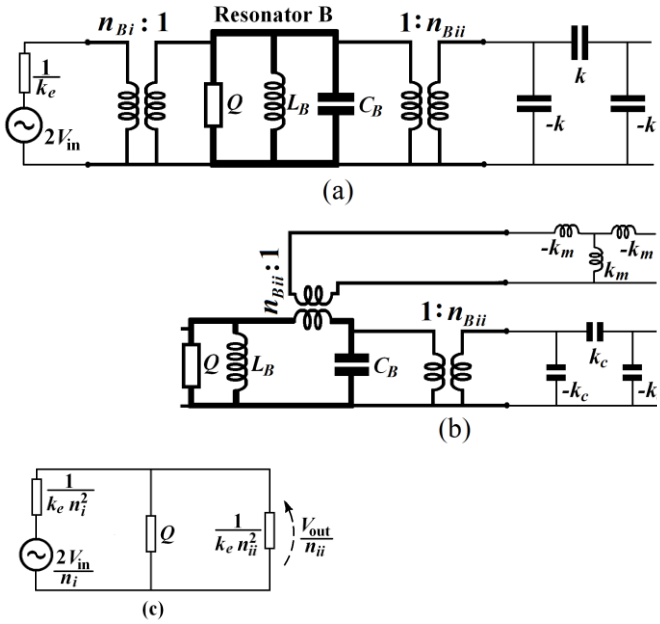

Fig. 5. Equivalent circuit for resonator B in a multi-order filter, together with input and impedance inverter leading to the rest of the circuit. (a) electric coupling only (b) mixed coupling; and (c) equivalent circuit at resonance of a single resonator.

TABLE I
ESTIMATED RESONANCE FREQUENCIES AND VOLTAGE DISTRIBUTIONS OF RESONATORS WITH STUBS

Main line: Z_m=72 Ω and $\lambda_1/2$=61mm .

d mm	Z_s ohms	Resonant Freq [a]		$n_{i\,(b)}$	$n_{ii\,(b)}$
8.5	50	f_{11}	0.96	1.07	0.80
		f_{21}	1.75	0.57	1.31
		f_{31}	2.45	1.12	0.26
		f_{32}	3.69	0.90	0.76
4	29.5	f_{11}	0.98	1.09	0.84
		f_{21}	1.50	0.59	1.15
		f_{31}	2.69	1.26	0.10
		f_{32}	3.39	0.12	1.41
6	123	f_{11}	0.99	1.03	0.94
		f_{21}	1.82	0.77	1.10
		f_{31}	2.65	1.07	0.31
		f_{32}	3.43	0.44	1.13
1.625	33.2	f_{11}	1.00	1.05	1.02
		f_{21}	1.49	0.76	0.98
		f_{31}	2.87	1.29	0.09
		f_{32}	3.15	0.09	1.36

(a) Resonant frequencies are normalized to the fundamental of the main line with no stub.
(b) Equivalent-circuit transformer ratios compared with a resonator with no stub.

The expected values of n_i and n_{ii} for the two prongs (i) and (ii) for the four cases considered in section II are given in table I, while the levels of the spurious peaks are compared with the simulation results in Fig. 4. (Subscript B has been omitted since there is only one resonator). The coplanar line inputs and outputs have an interaction over a very short distance, to avoid coupling to non-adjacent resonator prongs. For example, the interaction between the coplanar output and prong (i) in fig. 2 is very small even when the voltage redistribution brings about a large voltage in prongs (i) and (iii), and small voltage in prong (ii). The equivalent circuit at resonance is shown in fig. 5(c). L and C cancel so they are not drawn. Source and load as seen through the transformers have the values indicated. If Q is much smaller than the other two resistors,

$$\frac{V_{\text{out}}}{V_{\text{in}}} \approx 2 n_i n_{ii} k_e Q \qquad (12)$$

so the peaks are reduced relative to the resonator with no stubs by a factor $n_i n_{ii}$.

The estimated and simulated response levels in fig. 4 are similar, confirming that the estimate for the new external coupling is reasonable. The improvement in suppression is modest for the second order spurious response, but the third order spurious modes are decreased by between 3 and 19 dB. The dominant means of suppression is the stagger tuning, which is not visible here because single resonators are being considered. The unevenness in improvement can to some extent be adjusted by varying the stub length. This adjustment is also necessary because inductive and capacitive coupling between the stub and the main line makes the ideal stub length depart from a quarter of the third harmonic wavelength by up to 0.5 mm.

Further simulations were conducted to confirm both the internal and external coupling. The layout is given in fig. 6 for the 29 ohm stub; the 123 ohm spiral stub has a similar layout. The hairpins shown in fig. 6(a) are unfolded as in fig. 6(b) and 6(c). This reduces the unwanted coupling between non-adjacent prongs, for example between $A(ii)$ and $B(i)$. For the 29 ohm line, the tap junction is modified as shown to mitigate the current bottleneck. In fig. 6(b), the dimension 4 mm shows the distance between the tap and the centre of the main line. The input has close coupling to observe k_e, while a variable output line position at larger distance is chosen to have minimal influence. The value of k_e is found from the 3-dB bandwidth of S_{21}. In fig. 6(c), the value of k is found from the frequency difference between two peaks of S_{21}, that is, the antisymmetric and symmetric responses, divided by the mean value,

$$k \approx \frac{f_s - f_a}{0.5(f_s + f_a)} \qquad (13)$$

which is an approximation for

$$k = \frac{f_s^2 - f_a^2}{f_s^2 + f_a^2} \qquad (14)$$

The variation of coupling coefficient with transformer ratio is shown in fig. 7. The expected slopes agree with the new values of coupling coefficients, that is, $k_e\, n^2$ and $k\, n_A\, n_B$. (Subscripts A, (i) and (ii) are omitted where it is clear which

resonators or prongs are relevant). Coupling coefficients can be decreased very substantially. The importance of straightening the hairpins is shown in an extreme case before straightening, when A(*ii*) was topmost and B(*ii*) was on the bottom; the coupling at f_{32} between them was 2.8×10^{-3}, which dominates the values of *k* on the left hand side of fig. 7.

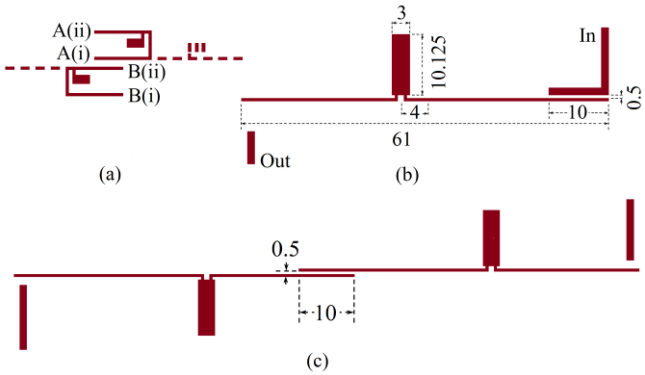

Fig. 6. Layout for simulations to verify the change of internal and external coupling coefficients. (a) Two coupled hairpins with stubs. (b) One straightened hairpin, to find k_e. (c) Two straightened hairpins, to find *k*.

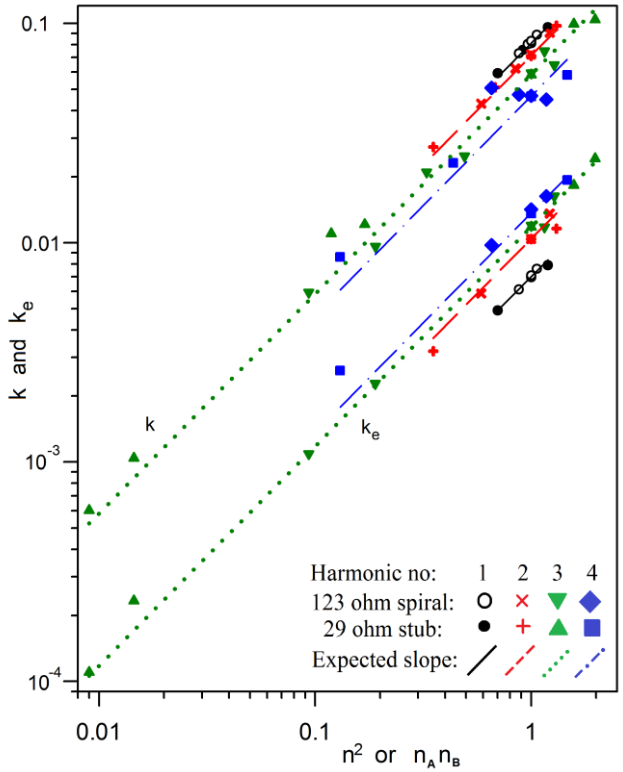

Fig. 7. Variation of internal and external coupling coefficient with turns ratio *n*. First harmonic is synonymous with the fundamental.

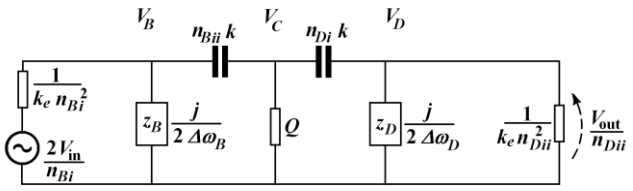

Fig. 8. Filter equivalent circuit, with the center resonator resonating.

IV. Filter Equivalent Circuit

At a spurious resonance of resonator *C*, normalized to 1, the equivalent circuit is as in fig. 8. The negative, parallel capacitors of the immitance inverters $-n_{Bii}k$ and $-n_{Di}k$ have been ignored. Resonators *B* and *D* are well off resonance, so their resistance has negligible effect. For *C*, the inductor and capacitor cancel, leaving resistor *Q*. Taking z_B, *Q* and z_D to be very small compared with the impedances of the other components,

$$V_B \approx \frac{j}{2\Delta\omega_B} k_e n_{Bi}^2 \frac{2V_{\text{in}}}{n_{Bi}} \qquad (15)$$

$$V_C \approx Q\, n_{Bii}\, k\, V_B \qquad (16)$$

$$V_D \approx \frac{j}{2\Delta\omega_D}\; n_{Di}\, k\, V_C \qquad (17)$$

which leads to

$$\left|\frac{V_{\text{out}}}{V_{\text{in}}}\right| \approx \frac{k_e k^2 n_{Bi} n_{Bii} n_{Di} n_{Dii} Q}{2\,\Delta\omega_B \Delta\omega_D} \qquad (18)$$

When resonator *B* or *D* is resonant, equations of the same form can be found, with $\Delta\omega_B$ and $\Delta\omega_D$ replaced by the difference between the input frequency and the resonant frequency of the non-resonant resonators.

This equation shows that the voltage redistributions reduce the spurious levels significantly, but it is not a good quantitative estimate for several reasons. The values of k_e and *k* taken from the original filters without stubs are not constant over the large bandwidth. The coupling between non-adjacent prongs of different resonators has already been seen to be significant, and not accounted for. *Q* may not be sufficiently small. Adjusting stub lengths to equalize the peaks may lead to a response which is better than predicted. Finally, fig. 8 only considers one mode of each resonator. In fig. 4, the responses of resonators with stubs clearly show a null near 3000 MHz, due to two modes cancelling.

V. Filter Simulations and Measurements

Filters with center frequency approximately 1 GHz and fractional bandwidths 22%, 15%, and 8% were designed. The stub lengths and tap positions for the first two filters were already available by trial and error before the foregoing analysis was formulated, but fig. 4 shows that the equations could have been used instead, to give evenly spaced peaks. Fig. 3 was used for the stubs in the 8% bandwidth filter, and confirmed to be appropriate by fig. 4. The additional suppression due to the current redistributions was simply accepted for the present filters; Z_s and *d* were not re-adjusted for an overall optimum. Because of the effects not incorporated in section IV, the equations can estimate the spurious levels only very crudely and they would probably have to be confirmed by simulations.

The substrate and the track width of the main lines of the resonators is the same as in section II. The other dimensions are given in Table II, with reference to fig. 1. Overall

dimensions of resonators A, …, E are m_A x 6 mm, ... m_E x 6 mm (only m_A is shown in fig. 1). The 6 mm excludes the small displacements f_{AB}, … f_{DE}, which bring the sections of length $l_{AB, \ldots} l_{DE}$ closer to the neighboring resonators. Varying l_{AB} allows fine tuning of the coupling coefficient without requiring very small cell sizes. The vertical distance between the bend in any resonator and the bend in a next neighbor is 28 mm. Stubs with higher characteristic impedance placed closer to the voltage node of the fundamental frequency were thought sufficient for the 8% bandwidth filter with its narrower harmonics. They perturb the fundamental response less.

The initial designs without stubs had responses with significant 2nd and 3rd harmonics. The stubs were added, and the gaps between resonators, the resonator lengths, and the stub lengths adjusted by manual iterations. For the filters with stubs, a lid was placed 10 mm above the substrate. In lieu of side-walls, conducting spacers were placed close to resonators *B*, *C*, and *D*. The lid and spacers were required to reduce direct coupling between resonators *A* and *E*. The filters with no stubs could be measured with no lid or spacers. A photograph of one of the filters is given in fig. 9.

Measured results and simulated results (using "SONNET" 0.125 mm cell size and "edge mesh") are shown in figs. 10-12. A very significant suppression of harmonics is evident (also in table II), even though they fall short of the -40 dB (and below) found from simulations. The estimates are poor, as already discussed. The highest spurious peaks sometimes merge with the fourth order spurious responses. Comparing filters with and without harmonic suppression, there is no discernible change in measured nor in simulated pass band attenuation beyond that expected from the slightly different bandwidths.

Measured S_{11} and S_{22} are also shown. There are some notches in the stop band close to the suppressed spurious resonances, in common with other results, including [5]. With resonator A damped by the input so it has a low Q factor, the S_{11} notches are related to absorption by resonator B at its resonant frequencies, since the transmission does not account for the energy loss, while radiation is small because of the enclosure. The resonances of C and D are shielded from the input by the low off-resonance response of B. The filter is neither symmetrical nor lossless in the stop band, so the S_{22} stop band notches are at different frequencies, and mainly due to resonator D. The 22% bandwidth filter has no S_{22} notches deeper than 0.5 dB until 3000 MHz; this may warrant further study. Power amplifiers, working in their non-linear regions almost as switches, may require low absorption by the filters at the harmonics. A feature of stagger tuning is that the notches can be shifted away from these harmonics.

Magnified views of the pass band responses are shown in figs. 13 and 14. The maximum pass band S_{11} and S_{22} are approximately -8 dB in the 22% filter, but better in the other two filters. The simulated values (not shown in the figures) are approximately -16dB, so there is a significant contribution due to fabrication error, and re-design and fabrication may be appropriate. The 22% and 15% filters which used the same resonators have similar S_{11} shapes, with the worst pass band maxima at higher frequencies, suggesting that the error could be repeatable and reliably removed in a second design.

VI. Conclusion

The 2nd and 3rd harmonics of microstrip filters have been successfully suppressed using stubs. Equations have been provided to determine the position of the stubs and their characteristic impedances. Measurements have shown good results. Work is now under way to combine this technique with other methods to attenuate more harmonics, and to consider dual-mode resonators, as a first step towards multimode resonators [28].

The suppression in some filters is given in table III. Selection is biased towards filters with large passband widths; coupling is usually stronger at the harmonics, which are a greater challenge to suppress. Some of the data were read off the small scale graphs presented, and are therefore approximate. Particularly noteworthy is [10], which has a wide pass band and good spurious suppression over a broad band. However, it requires fabrication of narrow lines. The filters with nearly uniform widths in the main lines are [24], [14], [22] and [23], but these only suppress the second harmonic, or need additional components, or have relatively narrow passband widths. The present work is therefore a useful addition to the techniques available.

TABLE II
Filter dimensions (mm), coupling coefficients before the addition of stubs, and spurious levels (dB)

Bandwidth (%)	22	15	8
m_A	26.625	26.875	27.5
m_B	27.375	26.875	27.75
m_C	27.625	27.5	27.75
m_D	28.625	27.875	28
m_E	26.75	26.875	27.5
e	6.375	5.25	3
g_{AB}	0.625	1.125	1.75
g_{BC}	0.5	1.125	2.125
g_{CD}	0.625	1.25	2.125
g_{DE}	0.625	1.25	1.75
l_{AB}	0	7	2
l_{BC}	NA	8.25	7
l_{CD}	5	9.5	4
l_{DE}	0	9.75	5
f_{AB},	$g_{AB} - 0.5$,	0.5	0.5
$f_{BC\ldots}$	$g_{BC} - 0.5$, …	0.5…	0.5…
s_B	9.75	8.875	Spiral: a= 2.38
w_B	1.25	1.25	b=1.25
d_B	8.5	8.5	6
s_D	10.25	10	9.25
w_B	3	3	2.5
d_D	4	4	1.625
Simulations, no stubs:			
2nd harm. k_e	0.018	0.010	0.005
k	0.060	0.054	0.041
3nd harm. k_e	0.003	0.006	0.003
k	0.050	0.056	0.013
Spurious levels, Estimated (dB)			
2nd harm.	-16 to -22	-23 to -29	-31 to -40
3rd harm.	-45 to -59	-38 to -51	-67 to -76
Worst Simulated (dB)	-41	-41	-39
Worst Measured (dB)	-37	-34	-36

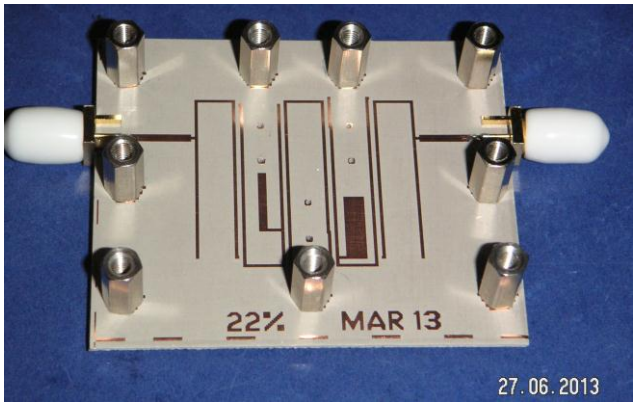

Fig. 9. The 22% bandwidth filter, with the cover removed. The dimensions are defined in fig. 1 and table II. 10 mm high posts form skeleton side walls similar to a substrate-integrated waveguide. In the 22% and 15% filter, both stubs are close to the center resonator C (defined in fig. 1), while in the 8% filter, the stub in resonator D was (accidentally) placed closer to resonator E (as in fig. 1) but with after iterative fine tuning, responses were not affected. The small holes within resonators *B*, *C*, and *D* are available to accept pins for more screening, but the improvement is marginal and the data will not be presented .

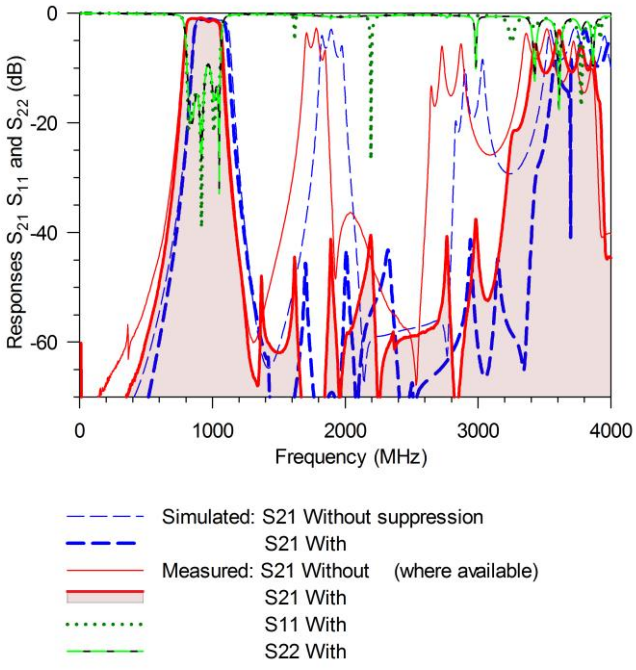

Fig. 10. 22% bandwidth filter response

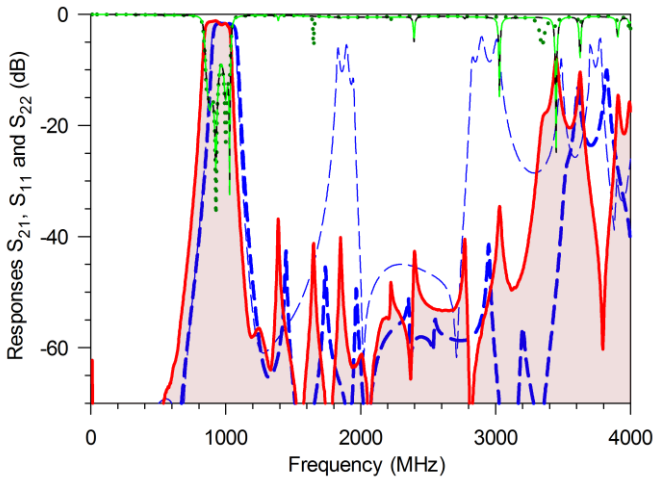

Fig. 11. 15% bandwidth filter response (see fig. 10 for legend). The original filter with no stubs was not fabricated.

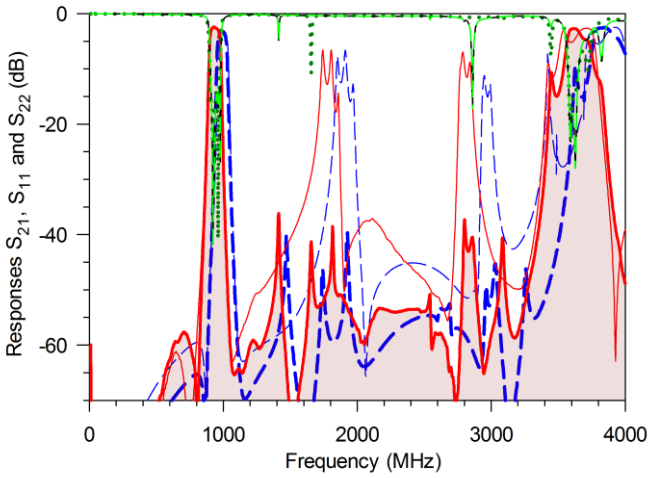

Fig. 12. 8% bandwidth filter response (see fig. 10 for legend).

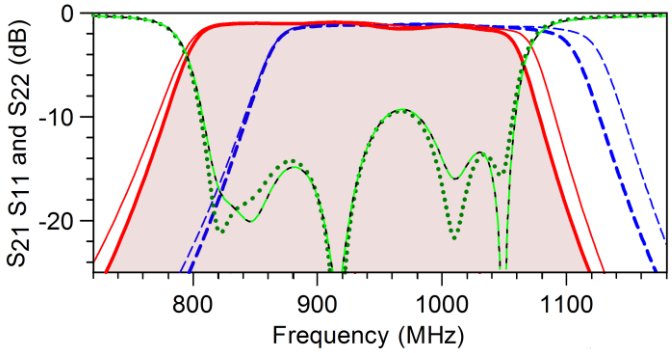

Fig. 13. Magnified plot of the 22% bandwidth filter pass band (see fig. 10 for legend).

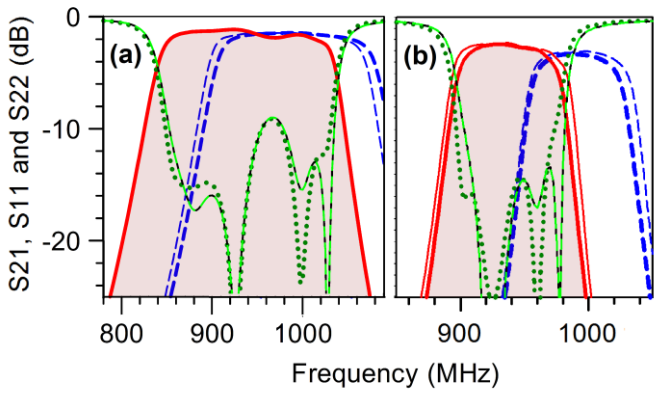

Fig. 14. Magnified plot of (a) the 15% (b) the 8% bandwidth filter pass bands (see fig. 10 for legend). The vertical scale applies to both graphs.

TABLE III
A SELECTION OF FILTERS WITH HARMONIC SUPPRESSION

2^{ND} HARMONIC SUPPRESSION

Ref	Mechanism	Band width (%)	Attenuation (dB)
[1]	Line width	30	48
[7]	Ground plane aperture	30	25
[24]	Resonator overlap	20	55

WIDE BAND SUPPRESSION

Ref	Mechanism	Band width (%)	Atten (dB)	Stop-band limit [(a)]
[5]	Wiggly line	10	30	6.5 f_1
[10]	Step impedance / capacitive loading	20	40	10 f_1
[14]	Resistors	10	29	3.9 f_1
[22]	Resonator overlap / capacitive loading	10	50	3.2 f_1
[23]	Resonator overlap	15	35	4.5 f_1
This work	Stubs	22	37	3.2 f_1

(a) The centre of the pass band is f_1.

REFERENCES

[1] J. Marimuthu and M. Esa, "Wideband and harmonic suppression method of parallel coupled microstrip bandpass filter using centered single groove", in *Proceedings of the 2007 IEEE International Conference on Telecommunications and Malaysia International Conference on Communications* , Penang, Malaysia, pp622-626, May 2007.

[2] T. Lopetegi, M.A.G. Laso, J. Hernandez, M. Bacaicoa, D. Benito, M. J. Garde, M. Sorolla and M. Guglielmi, "New microstrip "wiggly-line" filters with spurious passband suppression", *IEEE Trans. Microwave Theory and Techn.*, vol.49, no. 9, pp. 1593-1598, Sep. 2001.

[3] B. S. Kim, J. W. Lee and M. S. Song, "An implementation of harmonic-suppression microstrip filters with periodic grooves", *IEEE Microwave and Wireless Components Letters*, vol. 14, no.9, pp. 413-415, Sep. 2004.

[4] J.-T. Kuo, W.-H. Hsu and W.-T. Huang, "Parallel coupled microstrip filters with suppression of harmonic response", *IEEE Microwave and Wireless Components Letters*, vol. 12, no.10, pp. 383-385, Oct. 2002.

[5] T. Lopetegi, M.A.G. Laso, F. Falcone, F. Martin, J. Bonarche, J. Garcia, L. Perex-Cuevas, M. Sorolla and M. Guglielmi, "Microstrip "wiggly-line" bandpass filters with multi-spurious rejection", *IEEE Microwave and wireless components letters*, vol. 14, no. 11, pp. 531-533, Nov. 2004.

[6] R. Phromloungsri, M. Chongcheawchamnan, and I. D. Roberts, "Inductively compensated parallel coupled microstrip lines and their applications", *IEEE Trans. Microwave Theory and Techn.*, vol.54, no. 9, pp. 3571-3582, Sep. 2006.

[7] M. C. Velazques-Ahumada, J. Martel, and F. Medina, "Parallel coupled microstrip filters with ground-plane aperture for spurious band suppression and enhanced coupling", *IEEE Trans. Microwave Theory and Techn.*, vol. 52, no. 3, pp. 1082-1086, Mar. 2004.

[8] M. C. Velazques-Ahumada, J. Martel, and F. Medina, "Parallel coupled microstrip filters with floating ground-plane conductor for spurious band suppression", *IEEE Trans. Microwave Theory and Techn.*, vol. 53, no. 5, pp. 1823-1828, May. 2005.

[9] J. Garcia-Garcia, F. Martin, F Falcone, J. Bonache, J. D. Baena, I. Gil, E. Amat, T. Lopetegi, M.A.G. Laso, J. A. M. Iturnendi, M. Sorolla, and R. Marques, "Microwave filters with improved stopband based on sub-wavelength resonators", *IEEE Trans. Microwave Theory and Techn.*, vol. 53, no. 6, pp. 1997-2006, Jun. 2005.

[10] W. M. Fathelbab and M. B. Steer, "Parallel-coupled line filters with enhanced stopband performances", *IEEE Trans. Microwave Theory and Techn.*, vol.53, no. 12, pp. 3774-3781, Dec. 2005.

[11] M. Makimoto and S. Yamashita, "Bandpass filters using parallel coupled stripline stepped impedance resonators", *IEEE Trans. Microwave Theory and Techn.*, vol. MTT-28, no. 12, pp. 1413-1417, Dec. 1980.

[12] F. Huang, "Suppression of Superconducting Filter Spurious Response Using Lossy Parasitic Resonators", IET Microwaves, Antennas and Propagation, vol. 4, no. 12, pp. 2042-2049, Dec. 2010.

[13] F. Huang, "Suppression of Microstrip Filter Spurious Responses Using Frequency-Selective Resistive Elements", IET Microwaves, Antennas and Propagation, , vol. 5, no. 15, pp. 1836-1843, 2011

[14] F. Huang, "Suppression of Spurious Responses in Microstrip Filters Using a Reduced Number of Resistors" IET Microwaves, Antennas and Propagation, vol. 6, no. 10, pp. 1128-1135, Jul. 2012.

[15] P.-H. Deng, S.-C. Lin, Y.-S Lin, C.-H. Wang and C. H. Chen, "Microstrip bandpass filters with dissimilar resonators for suppression of spurious responses", in *Proceedings of the 35rd European Microwave Conference*, Paris, France, Oct. 2005, pp. II-1263-1266.

[16]C.-F. Chen, T.-Y. Huang, and R.-B. Wu, "Design of microstrip bandpass filters with multiorder spurious-mode suppression", IEEE Trans. Microwave Theory and Techn., vol. 53, no. 12, pp. 3788-3793. Dec 2005.

[17] M. Makimoto and S. Yamashita, "Half-wavelength-type SIR" in *Microwave resonators and filters for wireless communication*, Berlin: Springer Verlag, 2001. ISBN 9783642087004.

[18] W.-H. Tu, H. Li, K. A. Michalski and K. Chang, "Microstrip Open-Loop Ring Bandpass Filter Using Open Stubs for Harmonic Suppression", in IEEE MTT-S Int. Microw. Symp. Dig., San Francisco, 2006, pp 357-360.

[19] K.-W. Hsu, M.-J. Tsou, Y.-H. Tseng, and W.-H. Tu, "Wide-Stopband Bandpass Filter with Symmetrical Loaded-Stub Resonators", in Proceedings of the Asia-Pacific Microwave Conference, 2011, pp1043-1046.

[20] A. Griol, J. Marti and L. Sempere, "Microstrip multistage coupled ring bandpass filters using spur-line filters for harmonic suppression", *Electronics Letters*, vol. 37, no. 9, pp. 572-573, Apr. 2001.

[21] S. Hong and K. Chang, "A parallel-coupled microstrip bandpass filter with suppression of both the 2nd and the 3rd harmonic responses", in IEEE MTT-S Int. Microw. Symp. Dig., San Francisco, 2006, pp 365-368.

[22] P. Cheong, S.-W. Fok, and K.-W. Tam, "Miniaturized Parallel Couple-Line Bandpass Filter With Spurious-Response Suppression", *IEEE Trans. Microwave Theory and Techn.*, vol.53, no. 5, pp. 1810-1816, May 2005.

[23] M.A. Sanchez-Soriano, G. Torregrosa-Penalva and E. Bronchalo, "Multispurious Suppression in Parallel-Coupled Line Filters by Means of Coupling Control", IET Microwaves, Antennas and Propagation, vol. 6, no. 11, pp. 1269-1276, 2012

[24] J.-T. Kuo, S.-P. Chen, and M Jiang, "Parallel-coupled microstrip filters with over-coupled end stages for suppression of spurious responses", *IEEE Microwave and wireless components letters*, vol. 13, no. 10, pp. 440-442, Oct. 2003.

[25] W. Tang and J.-S. Hong, "Quasi-elliptic function doublet filters without cross coupling", Proceedings of the 39th European Microwave Conference, Rome, Sep/Oct. 2009, pp. 452-455.

[26] M. C. Velazquez-Ahumada, J. Martel, F. Medina, and F. Mesa, "Design of a dual band-pass filter using modified folded stepped-impedance resonators", 2009 IEEE MTT-S International Microwave Symposium Digest, Boston, 2009, pp. 857 – 860.

[27] P. Mondal and M. K. Mandal, "Design of Dual-band bandpass filters using stub-loaded open-loop resonators", *IEEE Trans. Microwave Theory and Techn.*, vol. 56, no. 1, pp. 150-155, Jan. 2008.

[28] L. Zhu, S. Sun, and W Menzel, "Ultra-wideband (UWB) bandpass filters using multiple-mode resonator", *IEEE Microwave and wireless components letters*, vol. 15, no. 11, pp. 796-798, Nov. 2005.

Frederick Huang received the B.A. and D. Phil degrees in Engineering Science from the University of Oxford in 1980, and 1984. Since 1989 he has been a lecturer with the University of Birmingham.

Previous research interests are surface acoustic wave (SAW) dot array pulse compressors, analogue voice scramblers, Langmuir-Blodgett films, SAW and superconducting linear phase and chirp filter synthesis using inverse scattering, slow-wave structures, superconducting quasi-lumped element filters, switched filters and delay lines, together with microstrip and waveguide discontinuities. The main current interests are spiral band-pass filters and filter harmonic suppression.

Dr. Huang is a member of the IET (UK).